# Optimization of a Perovskite-based Multilayer Microwave Absorber using an Equivalent Circuit Model

**Aayushi Arya**
Department of Electrical Engineering, Indian Institute of Technology Hyderabad, India
aayushi.arya1993@gmail.com
(corresponding author)

*Received: 22 December 2022 | Revised: 7 January 2023 | Accepted: 15 January 2023*

**ABSTRACT**

**In this paper, the optimization of a perovskite-based multi-layer microwave absorber is performed to find an optimized value of the impedance step gradient from the refractive index of the constitutive layers. The optimization presented is unique as it is based on maximizing the dissipation and attenuation ability of the absorber along with a constraint of providing an efficient reflection loss in the absorber. This type of approach ensures the maximum absorption rate of the incident EM waves as the penetrating waves get fully dissipated. Objective and constraint functions are derived from the equivalent circuit model of the multi-layer absorber. The equivalent circuit model is formed using the inductive and capacitive effects across the dielectric and magnetic properties of the constitutive layers. The three layers are composed of perovskite materials with different refractive indexes such that the top layer serves as an impedance-matching layer followed by an alternate dielectric and magnetic layer. It is further shown how the capacitive and inductive losses are dominant over each other in the alternate lossy layers. Empirical relations are used to tabulate the refractive index of a range of perovskite compounds from which suitable combinations can be selected as per the obtained value of the step gradient function. The current work presents a simplistic method to design multi-layer microwave absorbers with different material combinations that are beneficial to the practical applications of microwave absorbers.**

***Keywords-multi layer microwave absorber; equivalent circuit model; perovskite; refractive index***

## I. INTRODUCTION

Multilayer structures form an important part in the field of microwave absorption. While single layer absorbers may be sufficient for absorber coatings, in applications where heavy exposure of EM radiation is to be absorbed, multilayer absorbers are more efficient [1]. Researchers have used optimization-based approaches like Genetic Algorithm (GA), Particle Swarm Optimization (PSO), and other evolutionary algorithms to design multilayer absorbers using Chew's recursive formula [2-3]. However, the recursive formula used in the above algorithms presents a limitation on the analysis of the individual layers in the multilayer design. Carbon-based absorbers recursive formula was commonly used as the changes in the properties of each layer are marginal and the configuration of each layer is the same with the difference being only in the volume of fillers used. Now, with researchers relying more on the inorganic materials to be used as microwave absorbers, the analysis and modeling theories of multilayer absorbers should be adapted and usually, more prominently used in frequency selective surfaces equivalent circuit models, can help in designing much simplistic models for the optimization of multilayer absorbers [4-5].

In this work, an attempt has been made to analyze and optimize the design of multilayer absorbers. The optimization is done by developing an equivalent circuit model for a three-layer perovskite-based multilayer design. The model takes into account the capacitive and the inductive losses in the alternate dielectric and magnetic layers of the absorber and includes the characteristics and properties of the individual layers. Supporting theories have been provided to understand the role of each layer and the loss mechanism occurring at the alternate layers of the absorber. In the current work, an equivalent circuit model for multilayer absorber is formed by including the dissipation properties of each layer. The reason for choosing perovskite for the absorber design is its inherited dielectric and magnetic properties that can be tuned easily by just changing the composition of the oxide [6]. Hence, in this work an optimized design of a three-layer microwave absorber is presented with different perovskite oxide combination for the individual layers.

## II. EQUIVALENT CIRCUIT MODEL

Perovskite oxides are inorganic compounds with a basic composition of $ABO_3$ type where A and B are cations and O is oxygen. In microwave absorbing perovskite composites,

permittivity and permeability depend on the composition of the perovskite compound, the creation of defects, oxygen vacancies, and influence of cations on the boundary material [7-8].

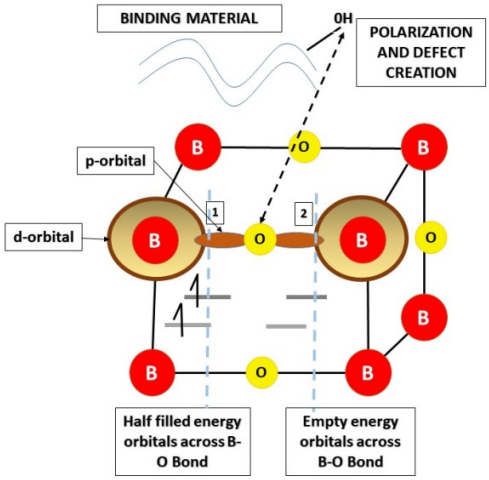


Fig. 1. Polarization and charge distribution in perovskite composite.

Permittivity and permeability of a perovskite are affected by different properties of the composite [9]. As shown in Figure 1, the permittivity of perovskites is determined mainly by the nature and amount of polarization occurring across the individual unit cell. Dipole and interfacial polarizations contribute mainly to the permittivity. These can be easily induced in a composite structure by using functionally active and oxygen interactive binding materials along with the perovskite filler. Graphene and reduced graphene oxide form one such example [10]. The interaction between the oxygen in the unit cell and the functional group of the binding material creates vacancies and defects thereby increasing the overall permittivity. Similarly, for induced permeability, charge distribution across the B-O-B bond of perovskite plays an important role. In the B-O-B bond of the perovskite p-orbital of oxygen overlaps with the d-orbital of the B cation on both sides, such that the bond is split to an upper and lower energy orbital. If the charge distribution is such that one of the upper energy levels is half filled for one B-O bond while the other on the opposite side is empty, magnetic dipoles get induced across the perovskite unit cell [11-13]. This charge distribution is also affected by the boundary material used in the composite. Based on the above explanation, it can be concluded that permittivity and permeability show trade off characteristics in magnetic and dielectric perovskite composites. Theoretically, this can be understood by considering that in order to have a higher permittivity, the interaction of the oxygen anion with the binding material must increase to create higher polarization. This in turn will weaken the B-O-B bond leading to lower the magnetic charge interaction across the B-O-B bonds decreasing permeability. Hence, in lieu of the above theory presented, maximum amount of dissipation losses can be obtained if separate layers for dielectric and magnetic losses can be combined alternately in multilayer absorbers with the top layer serving as an impedance matching layer to minimize the reflection loss. This will not only provide the required reflection loss, but also an efficient dissipation mechanism. Using alternate layers of dielectric and magnetic compounds can also reduce the risk of interference when using microwave absorbers in practical applications with devices that are dielectric or magnetic.

In order to formulate an objective function, the equivalent circuit model of Figure 2 is presented, which is based on the dissipation theory explained above. Two objective functions are formulated: one for the overall reflection loss and another for the net dissipation in the absorber. In Figure 2, the first layer provides the impedance matching, with the input impedance of the layer matched with the free space impedance to allow the maximum amount of microwaves to penetrate across the composite with reflection loss less or equal to -20dB as per industrial standards. Below the top layer, there are the dielectric and magnetic dissipation layers represented as lumped capacitor and inductor respectively. In the dielectric layer, dissipation occurs via the formation of dielectric dipoles across the layer [14]. The dipoles are aligned in such a way that the upper layer intersection is positively charged, while the lower is negatively charged and can be shown as a lumped capacitor in the circuit model. The incident microwave charge is stored and dissipated across this capacitor. The third layer is magnetic with the dissipation occurring due to the formation of magnetic dipoles across the layer [15]. The magnetic dipoles are aligned in such a way that the magnetic lines generated due to the dipoles are directed towards the negative intersection of the capacitive layer. The current direction across the layer falls along the negative $x$ axis. Thus the impedance in the magnetic layer is represented as negative induction.

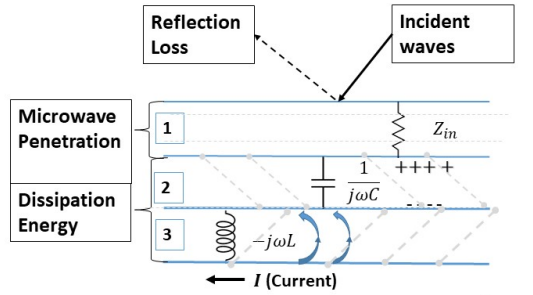


| Layer | Description |
|---|---|
| 1 | Impendence Matching Layer |
| 2 | Dissipative Layer Capacitive/ Dielectric |
| 3 | Dissipative Layer Inductive/ Magnetic |

Fig. 2. Equivalent circuit model of the multilayer microwave absorber.

## III. OBJECTIVE FUNCTIONS

The objective functions for the multilayer absorber are formulated to find an optimized value of the step gradient by which the refractive index of the consequent layers must increase from the top layer. Let $z$ be the value of the step gradient and $n$ be the value of the refractive index of the top layer. $L$ and $C$ are assumed to be the lumped inductance and capacitance of the magnetic and dielectric layer of the absorber composite given by [16]:

$$L = \mu\frac{Z}{\eta} \text{ and } C = \varepsilon\frac{\eta}{Z} \quad (1)$$

where $\eta$ is the characteristic impedance of the absorber and $Z$ is the input impedance of the absorber. The attenuation constant $\alpha_a$ of the absorber composite is given by:

$$\alpha_a = \frac{1}{2}G'Z \quad (2)$$

where $G'$ represents the imaginary part of the conductance in the equivalent circuit model. The conductance $G'$ can be presented in terms of $L$ and $C$ as:

$$G' = \frac{-1}{j\omega L} + j\omega C \quad (3)$$

where $\omega$ is the angular frequency. With $f$=2.54×10$^9$Hz, the angular frequency is given by $\omega$=2π$f$=1.59×10$^{10}$/rad/s. Combining (1)-(3), the following equation is obtained:

$$f_1 = (1 + \omega^2 LC)Z \quad (4)$$

Substituting $L$, $C$ from the above equations, (5) is obtained:

$$LC = \sqrt{\mu\varepsilon} = z.n \quad (5)$$

where $n$ is the refractive index value of the absorber composite and $z$ is the step gradient value, which is the input variable in the presented model. Now reversing $f_1$ for minimization, the objective function is given by:

$$min.f_1 = -(1 + \omega^2 zn)Z \quad (6)$$

For the second objective function, Reflection Loss (*RL*) coefficient for the absorber composite is considered [17]:

$$RL = \left|\frac{Z_{in} - Z_o}{Z_{in} + Z_o}\right| \quad (7)$$

The input impedance of the absorber can be written as:

$$Z_{in} = \eta\, tanh\left(\frac{\sqrt{\mu\varepsilon}2\pi f}{d}\right) \quad (8)$$

$Z_o$ is the characteristic impedance of free space. For an efficient amount of absorption in the absorber, the characteristic impedance of the microwave absorber $\eta$ must be such that *RL* must not be less than -20dB. To obtain the above value, $\eta$ must be related to $Z_o$ as [18]:

$$\eta = 1.22Z_o \quad (9)$$

Similarly, to optimize the function for reflection loss in terms of the refractive index, thickness is considered constant to simplify the objective function with:

$$d = 2\pi f \quad (10)$$

Substituting (8)-(10) in (7) and assuming tanh$x \approx x$ for small values of $x$, the function $f_2$ for optimizing the *RL* coefficient can be written as:

$$f_2 = \frac{1.22zn - 1}{1.22zn + 1} \quad (11)$$

$f_2$ represents the reflection coefficient of the absorber which depends on the required *RL* of the absorber as:

$$f_2 = \frac{10^{RL}}{20} \quad (12)$$

Solving (12) for the *RL* range from -20 to -60dB, the constraint equality for $f_2$ function comes out to be:

$$0.1 < f_2 < 0.7 \quad (13)$$

## IV. DATASET

The dataset for the refractive index of various perovskite oxides is created using an empirical relation between the spatial energy parameter, pseudo lattice constant, and the refractive index of the perovskite oxide. The spatial energy parameter depends on the polarization ability of the elements and the refractive index of the compound. Further, the polarization ability of a perovskite oxide is affected by all its compositional elements. Hence, the effective spatial energy is the sum of the individual polarization energy. The refractive index can be empirically calculated from the effective spatial energy and the lattice constant of the compound as follows:

$$n_2 = n \times \left(\frac{z}{2}\right) \quad (14)$$

The lattice constant of the perovskite oxide is taken from [19] and the polarization energy parameter from [18]. $P_{Ea}$ ,$P_{Eb}$ ,$P_{Eo}$ represent the polarization energy parameter in eV of cations A and B and oxygen as anion respectively. $\sum P_E$ is the effective spatial energy parameter, $r_o$ is the pseudo cubic lattice constant in Å and $n$ is the calculated refractive index. Table I provides the above parameters for different perovskite compounds.

## V. OPTIMIZATION-MULTI OBJECTIVE PSO

In the current study, multi-objective optimization is used for optimizing the step gradient for the refractive index value of the microwave absorber composite. In the presented model $f_1$ is minimized, while $f_2$ is optimized using the equality constraint. For carrying out the optimization, the object oriented framework is used involving the NSGA-II evolutionary algorithm. NSGA-II has the advantage of providing fast computations and a non-dominated solution set. It is one of the most popularly used GAs which uses the fitness value or the rank of an individual along with the assigned crowded distance to sort out individuals from consecutive generations. It uses the binary crossover operator for mutation and offspring generation. The algorithmic parameters used in the current study are an initial population of 50, 10 offspring in each generation, and termination at the 40$^{th}$ generation. The algorithm is repeated for an initial refractive index range of 1.6 to 2.3. The coding was executed using python in a PC with Intel(R) Core(TM) i5-8265U (CPU 1.60GHz) processor with 8GB RAM.

## VI. RESULTS

Using the step gradient value and the refractive index value of the top layer, the refractive indices for each layer can be determined as shown above. Suitable compounds as per the calculated values, having the same refractive index value, are picked from Table I. Table II shows the step gradient value obtained for each refractive index value along with possible multi-layer combinations matched from the data in Table I.

TABLE I. SPATIAL ENERGY PARAMETER AND REFRACTIVE INDICES OF VARIOUS PEROVSKITE OXIDES

| Compound | $P_{Ea}$ | $P_{Eb}$ | $P_{Eo}$ | $r_o$ | $\Sigma P_E$ | $n$ |
|---|---|---|---|---|---|---|
| $BaFeO_3$ | 0.271 | 1.285 | 6.287 | 4.102 | 7.843 | 1.91 |
| $BaMoO_3$ | 0.271 | 0.619 | 6.287 | 4.177 | 7.177 | 1.72 |
| $BaNbO_3$ | 0.271 | 0.562 | 6.287 | 4.212 | 7.12 | 1.69 |
| $BaSnO_3$ | 0.271 | 1.393 | 6.287 | 4.223 | 7.951 | 1.88 |
| $BaHO_3$ | 0.271 | 6.728 | 6.287 | 4.246 | 13.286 | 3.13 |
| $BaZrO_3$ | 0.271 | 0.507 | 6.287 | 4.258 | 7.065 | 1.66 |
| $BaIrO_3$ | 0.271 | 10.411 | 6.287 | 4.148 | 16.969 | 4.09 |
| $BaPbO_3$ | 0.271 | 0.867 | 6.287 | 4.322 | 7.425 | 1.72 |
| $BaTbO_3$ | 0.271 | 2.848 | 6.287 | 4.304 | 9.406 | 2.19 |
| $BaPrO_3$ | 0.271 | 0.82 | 6.287 | 4.408 | 7.378 | 1.67 |
| $BaCeO_3$ | 0.271 | 0.607 | 6.287 | 4.432 | 7.165 | 1.62 |
| $BaTiO_3$ | 0.271 | 0.889 | 6.287 | 4.125 | 7.447 | 1.81 |
| $BaRuO_3$ | 0.271 | 0.743 | 6.287 | 4.42 | 7.301 | 1.65 |
| $SrMnO_3$ | 0.413 | 1.174 | 6.287 | 3.841 | 7.874 | 2.05 |
| $SrVO_3$ | 0.413 | 0.966 | 6.287 | 3.899 | 7.666 | 1.97 |
| $SrFeO_3$ | 0.413 | 1.285 | 6.287 | 3.905 | 7.985 | 2.04 |
| $SrTiO_3$ | 0.413 | 0.889 | 6.287 | 3.928 | 7.589 | 1.93 |
| $SrTcO_3$ | 0.413 | 0.679 | 6.287 | 3.975 | 7.379 | 1.86 |
| $SrMoO_3$ | 0.413 | 0.619 | 6.287 | 3.98 | 7.319 | 1.84 |
| $SrNbO_3$ | 0.413 | 0.562 | 6.287 | 4.015 | 7.262 | 1.81 |
| $SrSnO_3$ | 0.413 | 1.393 | 6.287 | 4.027 | 8.093 | 2.01 |
| $SrHfO_3$ | 0.413 | 6.728 | 6.287 | 4.05 | 13.428 | 3.32 |
| $SrTbO_3$ | 0.413 | 2.848 | 6.287 | 4.108 | 9.548 | 2.32 |
| $SrCoO_3$ | 0.413 | 1.402 | 6.287 | 3.841 | 8.102 | 2.11 |
| $SrZrO_3$ | 0.413 | 0.501 | 6.287 | 4.061 | 7.201 | 1.77 |
| $SrRuO_3$ | 0.413 | 0.743 | 6.287 | 4.015 | 7.443 | 1.85 |
| $CaVO_3$ | 0.727 | 0.966 | 6.287 | 3.784 | 7.98 | 2.11 |
| $CaZrO_3$ | 0.727 | 6.728 | 6.287 | 3.934 | 13.742 | 3.49 |
| $CaHfO_3$ | 0.727 | 0.507 | 6.287 | 3.946 | 7.521 | 1.91 |
| $CaRuO_3$ | 0.727 | 0.743 | 6.287 | 3.899 | 7.757 | 1.99 |
| $CaSnO_3$ | 0.727 | 1.393 | 6.287 | 3.911 | 8.407 | 2.15 |
| $CaTiO_3$ | 0.727 | 0.889 | 6.287 | 3.813 | 7.903 | 2.07 |
| $EuTiO_3$ | 2.036 | 0.889 | 6.287 | 3.801 | 9.212 | 2.42 |
| $EuAlO_3$ | 2.036 | 1.767 | 6.287 | 3.643 | 10.09 | 2.77 |
| $EuCrO_3$ | 2.036 | 1.067 | 6.287 | 3.736 | 9.39 | 2.51 |
| $EuFeO_3$ | 2.036 | 1.285 | 6.287 | 3.771 | 9.608 | 2.55 |
| $EuGaO_3$ | 2.036 | 1.821 | 6.287 | 3.742 | 10.144 | 2.71 |
| $EuInO_3$ | 2.036 | 1.062 | 6.287 | 3.593 | 9.385 | 2.61 |
| $CeAlO_3$ | 0.607 | 1.767 | 6.287 | 3.771 | 8.661 | 2.3 |
| $GdAlO_3$ | 2.426 | 1.767 | 6.287 | 3.631 | 10.48 | 2.89 |
| $GdCrO_3$ | 2.426 | 1.067 | 6.287 | 3.725 | 9.78 | 2.63 |
| $GdFeO_3$ | 2.426 | 1.285 | 6.287 | 3.76 | 9.998 | 2.66 |
| $LaAlO_3$ | 0.418 | 1.767 | 6.287 | 3.795 | 8.472 | 2.23 |
| $LaCrO_3$ | 0.418 | 1.067 | 6.287 | 3.888 | 7.772 | 2 |
| $LaFeO_3$ | 0.418 | 1.285 | 6.287 | 3.923 | 7.99 | 2.04 |
| $LaGaO_3$ | 0.418 | 1.821 | 6.287 | 3.894 | 8.526 | 2.19 |
| $LaRhO_3$ | 0.418 | 0.799 | 6.287 | 3.947 | 7.504 | 1.9 |
| $LaTiO_3$ | 0.418 | 0.889 | 6.287 | 3.953 | 7.594 | 1.92 |
| $LaVO_3$ | 0.418 | 0.966 | 6.287 | 3.917 | 7.671 | 1.96 |
| $LaInO_3$ | 0.418 | 1.062 | 6.287 | 4.105 | 7.767 | 1.89 |
| $NdAlO_3$ | 1.074 | 1.767 | 6.287 | 3.689 | 9.128 | 2.47 |
| $NdGaO_3$ | 1.074 | 1.821 | 6.287 | 3.789 | 9.182 | 2.42 |
| $NdInO_3$ | 1.074 | 1.062 | 6.287 | 3.999 | 8.423 | 2.11 |
| $NdCoO_3$ | 1.074 | 1.402 | 6.287 | 3.701 | 8.763 | 2.37 |
| $NdCrO_3$ | 1.074 | 1.067 | 6.287 | 3.783 | 8.428 | 2.23 |
| $NdFeO_3$ | 1.074 | 1.285 | 6.287 | 3.818 | 8.646 | 2.26 |
| $NdMnO_3$ | 1.074 | 1.174 | 6.287 | 3.818 | 8.535 | 2.24 |
| $PrAlO_3$ | 0.82 | 1.767 | 6.287 | 3.725 | 8.874 | 2.38 |
| $PrCrO_3$ | 0.82 | 1.067 | 6.287 | 3.818 | 8.174 | 2.14 |
| $PrFeO_3$ | 0.82 | 1.285 | 6.287 | 3.853 | 8.392 | 2.18 |
| $PrGaO_3$ | 0.82 | 1.821 | 6.287 | 3.824 | 8.928 | 2.33 |
| $PrMnO_3$ | 0.82 | 1.174 | 6.287 | 3.853 | 8.281 | 2.15 |
| $PrVO_3$ | 0.82 | 0.966 | 6.287 | 3.847 | 8.073 | 2.1 |
| $SmAlO_3$ | 1.681 | 1.767 | 6.287 | 3.654 | 9.735 | 2.66 |
| $SmCoO_3$ | 1.681 | 1.402 | 6.287 | 3.666 | 9.37 | 2.56 |
| $SmVO_3$ | 1.681 | 0.966 | 6.287 | 3.777 | 8.934 | 2.37 |
| $SmFeO_3$ | 1.681 | 1.285 | 6.287 | 3.783 | 9.253 | 2.45 |
| $YAlO_3$ | 0.455 | 1.767 | 6.287 | 3.608 | 8.509 | 2.36 |
| $YCrO_3$ | 0.455 | 1.067 | 6.287 | 3.701 | 7.809 | 2.11 |
| $YFeO_3$ | 0.455 | 1.285 | 6.287 | 3.736 | 8.027 | 2.15 |

TABLE II. SUGGESTED COMPOUND LAYERS AS PER THE OBTAINED STEP GRADIENT VALUES

| Refractive index $n$ | Step gradient value $z$ | Suggested compound layers | | |
|---|---|---|---|---|
| 1.6 | 2.9 | $BaCeO_3$ | $CaHfO_3$ | $BaHfO_3$ |
| 1.7 | 2.8 | $BaPbO_3$ | $EuTiO_3$ | $SrHfO_3$ |
| 1.8 | 2.6 | $SrNbO_3$ | $SrTbO_3$ | $GdAlO_3$ |
| 1.9 | 2.5 | $SrTiO_3$ | $NdGaO_3$ | $GdAlO_3$ |
| 2 | 2.3 | $LaCrO_3$ | $CeAlO_3$ | $GdCrO_3$ |
| 2.1 | 2.2 | $CaVO_3$ | $CeAlO_3$ | $EuFeO_3$ |
| 2.2 | 2.1 | $LaAlO_3$ | $PrGaO_3$ | $SmVO_3$ |
| 2.3 | 2 | $SrTO_3$ | $PrGaO_3$ | $CeAlO_3$ |

## VII. CONCLUSION

The present work emphasizes on the importance of the use of materials' intrinsic electromagnetic properties in the designing of multilayer microwave absorbers. The provided theoretical framework gives a picture of the way the internal phenomenon of absorption and dissipation in absorbers can affect the output performance parameters. This understanding helps in building mathematical relations and functions which serve as building blocks to advanced computation procedures such as the used optimization. Moreover, the provided database from which perovskite compounds can be selected based on their refractive indices gives a wide range of options for designing and using unconventional combinations of materials as absorbers. The simplistic approach provided here can give more flexibility in the analysis of multilayer microwave absorbers.

## REFERENCES

[1] H. A. El-Hakim and K. R. Mahmoud, "Design of compact multi-layer microwave absorber for ultra-wide band applications thru shaping and RAM technologies," *Journal of Instrumentation*, vol. 14, no. 09, Jun. 2019, Art. no. P09006, https://doi.org/10.1088/1748-0221/14/09/P09006.

[2] M. Asi and N. I. Dib, "Design of Multilayer Microwave Broadband Absorbers Using Central Force Optimization," *Progress In Electromagnetics Research B*, vol. 26, pp. 101–113, 2010, https://doi.org/10.2528/PIERB10090103.

[3] M. H, M. V, and N. D. M, "Design of Microwave Absorbers using Improvised Particle Swarm Optimization Algorithm," *Journal of Microwaves, Optoelectronics and Electromagnetic Applications*, vol. 17, pp. 188–200, Jun. 2018, https://doi.org/10.1590/2179-10742018v17i2836.

[4] F. Costa, S. Genovesi, A. Monorchio, and G. Manara, "A Circuit-Based Model for the Interpretation of Perfect Metamaterial Absorbers," *IEEE Transactions on Antennas and Propagation*, vol. 61, no. 3, pp. 1201–1209, Mar. 2013, https://doi.org/10.1109/TAP.2012.2227923.

[5] S. Mallavarapu and A. Lokam, "Circuit Modeling and Analysis of Wearable Antennas on the Effect of Bending for Various Feeds," *Engineering, Technology & Applied Science Research*, vol. 12, no. 1, pp. 8180–8187, Feb. 2022, https://doi.org/10.48084/etasr.4699.

[6] A. Arya and G. V. V. Sharma, "Modelling of Microwave Absorption in Pervoskite Based Compounds Using Machine Learning Tools," in *Innovations in Electrical and Electronic Engineering*, Singapore, 2022, pp. 248–253, https://doi.org/10.1007/978-981-19-1677-9_21.

[7] Z. Gao, Z. Jia, J. Zhang, A. Feng, Z. Huang, and G. Wu, "Tunable microwave absorbing property of LaxFeO3/C by introducing A-site cation deficiency," *Journal of Materials Science: Materials in Electronics*, vol. 30, no. 14, pp. 13474–13487, Jul. 2019, https://doi.org/10.1007/s10854-019-01715-0.

[8] H. Ohsato, "Microwave Dielectrics with Perovskite-Type Structure," in *Microwave Dielectrics with Perovskite-Type Structure*, L. Pan and G. Zhu, Eds. IntechOpen, 2016, https://doi.org/10.5772/61718.

[9] S. Boumous, S. Belkhiat, and F. Kharchouche, "MgO Effect on The Dielectric Properties of BaTiO3," *Engineering, Technology & Applied Science Research*, vol. 9, no. 3, pp. 4092–4099, Jun. 2019, https://doi.org/10.48084/etasr.2705.

[10] S. Dai, B. Quan, B. Zhang, X. Liang, and G. Ji, "Interfacial polarizations induced by incorporating traditional perovskites into reduced graphene oxide (RGO) for strong microwave response," *Dalton Transactions*, vol. 48, no. 7, pp. 2359–2366, Feb. 2019, https://doi.org/10.1039/C8DT04966A.

[11] A. E. Irmak, "Structural and Electrical Properties of Ca2+ Doped LaFeO3: The Effect of A-site Cation Size Mismatch," *Engineering, Technology & Applied Science Research*, vol. 10, no. 2, pp. 5538–5546, Apr. 2020, https://doi.org/10.48084/etasr.3443.

[12] R. Schmidt, E. Langenberg, J. Ventura, and M. Varela, "Bi Containing Multiferroic Perovskite Oxide Thin Films," in *Crystallography, Chemistry and Catalytic Performance*, J. Zhang and H. Li, Eds. Nova Science Publishers, 2013.

[13] J. Y. Shin and J. H. Oh, "The microwave absorbing phenomena of ferrite microwave absorbers," *IEEE Transactions on Magnetics*, vol. 29, no. 6, pp. 3437–3439, Aug. 1993, https://doi.org/10.1109/20.281188.

[14] A. Prokopchuk, I. Zozulia, Y. Didenko, D. Tatarchuk, H. Heuer, and Y. Poplavko, "Dielectric Permittivity Model for Polymer–Filler Composite Materials by the Example of Ni- and Graphite-Filled Composites for High-Frequency Absorbing Coatings," *Coatings*, vol. 11, no. 2, Feb. 2021, Art. no. 172, https://doi.org/10.3390/coatings11020172.

[15] H. Schippers, T. Lundin, and J. Heijstek, "Modelling of magnetic radar absorbing composites," in *2010 URSI International Symposium on Electromagnetic Theory*, Berlin, Germany, Dec. 2010, pp. 596–599, https://doi.org/10.1109/URSI-EMTS.2010.5637158.

[16] P. C. Magnusson, V. K. Tripathi, and G. C. Alexander, *Transmission Lines and Wave Propagation, Third Edition*, 3rd ed. Boca Raton, FL, USA: CRC Press, 1991.

[17] Y. Liu, K. Zhao, M. G. B. Drew, and Y. Liu, "A theoretical and practical clarification on the calculation of reflection loss for microwave absorbing materials," *AIP Advances*, vol. 8, no. 1, Jan. 2018, Art. no. 015223, https://doi.org/10.1063/1.4991448.

[18] A. Arya and G. V. V. Sharma, "Prediction of material composition for microwave absorption through mathematical modelling," *Journal of Physics Communications*, vol. 5, no. 12, Sep. 2021, Art. no. 125002, https://doi.org/10.1088/2399-6528/ac37a7.

[19] A. S. Verma and V. K. Jindal, "Lattice constant of cubic perovskites," *Journal of Alloys and Compounds*, vol. 485, no. 1, pp. 514–518, Oct. 2009, https://doi.org/10.1016/j.jallcom.2009.06.001.